

Two-Channel Method for OTA Performance Measurements of MIMO-Enabled Devices

White paper

Products:

- | R&S®TS8991
- | R&S®AMS32
- | R&S®CMW500

Modern wireless communication technologies such as LTE, HSPA+ and WiMAX include the MIMO technology to achieve increased speed for data transmission. Existing Over-the-air (OTA) test systems need to be upgraded to support MIMO as well.

This white paper summarizes a straightforward and cost-effective approach to verify the OTA performance of MIMO-enabled devices. Measurements of receiver sensitivity and throughput are evaluated with statistical metrics.

Table of Contents

1	Introduction	4
2	Principles of R&S MIMO Test Proposal.....	5
2.1	Basics of MIMO operation	5
2.2	Split of MIMO measurements	7
3	Theoretical Model of the R&S MIMO OTA Test Proposal....	9
3.1	Static MIMO model	9
3.2	Antenna receiving patterns in static MIMO model.....	10
3.3	The two-channel method	12
4	Test plan for MIMO OTA measurements	15
4.1	Test case definition.....	15
4.2	Noise-limited OTA performance in transmit diversity mode	15
4.2.1	Goal of the test case	15
4.2.2	Settings for signal routing and the eNodeB emulator	16
4.2.3	Sensitivity threshold search	17
4.2.4	Measurement at single geometrical constellation	18
4.2.5	Variation of geometrical constellations.....	18
4.2.6	Evaluation of the figure of merit	19
4.2.7	Using CSI information	19
4.3	Peak performance measurements in spatial multiplexing mode.....	20
4.3.1	Goal of the test case.....	20
4.3.2	Settings for signal routing and the eNodeB emulator	20
4.3.3	Measurement at single geometrical constellation	21
4.3.4	Variation of geometrical constellations.....	22
4.3.5	Evaluation of the figure of merit	22
5	Test site characteristics and UE setup	23
5.1	UE coordinate system.....	23
5.2	Set-up with antennas in a vertical plane	23
5.3	Set-up with antennas in a horizontal plane	24
5.4	Calibration of the test set-up.....	25
5.5	UE set-up.....	26
5.5.1	General considerations and phantoms	26

5.5.2	Operation condition of the notebook.....	26
6	MIMO OTA System Implementation.....	27
6.1	System overview	27
6.2	OTA test chamber with internal components.....	27
6.3	External system components	28
7	Measurement Results	30
7.1	Summary of 3GPP round robin test with LTE devices	30
7.2	Noise-limited performance in transmit diversity mode.....	31
7.2.1	Example of LTE Transmit diversity measurement result	31
7.3	Peak performance measurements in spatial multiplexing mode	32
7.3.1	Example of OL spatial multiplexing measurement result.....	32
8	Conclusions.....	33
9	Abbreviations	34
10	References.....	35

1 Introduction

Internet-based services require increasing network performance for mobile applications. To meet this demand the evolution of wireless standards has added the Multiple-Input Multiple-Output (MIMO) techniques which improve data transfer capacity and reliability. Among various MIMO transmission modes spatial multiplexing is used to increase the channel capacity whereas transmit or receive diversity is used to increase the channel reliability for the allocated frequency spectrum.

Over-the-Air (OTA) performance measurements are an essential part of the certification test of wireless devices. Within an anechoic environment the radiated 3D pattern of both output power and receiver sensitivity are measured. Currently OTA performance tests for Single-Input Single-Output (SISO) are standardized for 2G, 3G and WLAN 802.11a,b,g devices. The figures of merit are the Total Radiated Power (TRP) and the Total Isotropic Sensitivity (TIS) as specified by CTIA [1], and similarly by 3GPP.

In principle such a test can also be applied to MIMO devices to evaluate the sensitivity threshold [2]. This updated version of the MIMO OTA white paper introduces statistical metrics of measurement results obtained in a 3D evaluation.

The two-channel method described in this white paper presents a straightforward and cost-effective approach for verification of the OTA performance on MIMO devices. Theoretical background of the method was presented in [3] with the objective to develop a test system and record measurement results presented in [7] to [11]. Since downlink (DL) 2×2 MIMO testing for spatial multiplexing and transmit diversity have the highest attraction at the moment, we are focusing on these transmission modes.

Section 2 describes the basics of the R&S MIMO test proposal.

Section 3 outlines the theoretical background of the proposed measurement principle.

Section 4 describes the test plan for MIMO OTA measurements with two basic test cases.

Section 5 shows the basic test site characteristics and how to calibrate it.

Section 6 describes the system architecture of a MIMO OTA test system for the two-channel method.

Section 7 shows measurement results of LTE modems with statistical metrics.

Section 8 concludes this white paper.

2 Principles of R&S MIMO Test Proposal

2.1 Basics of MIMO operation

In order to increase the channel capacity and reliability multiple antennas at both the transmitter and the receiver side are used. The environment with its multipath propagation is an integral part of the transmission, which allows separation of the simultaneous data streams at the receiver (Figure 1).

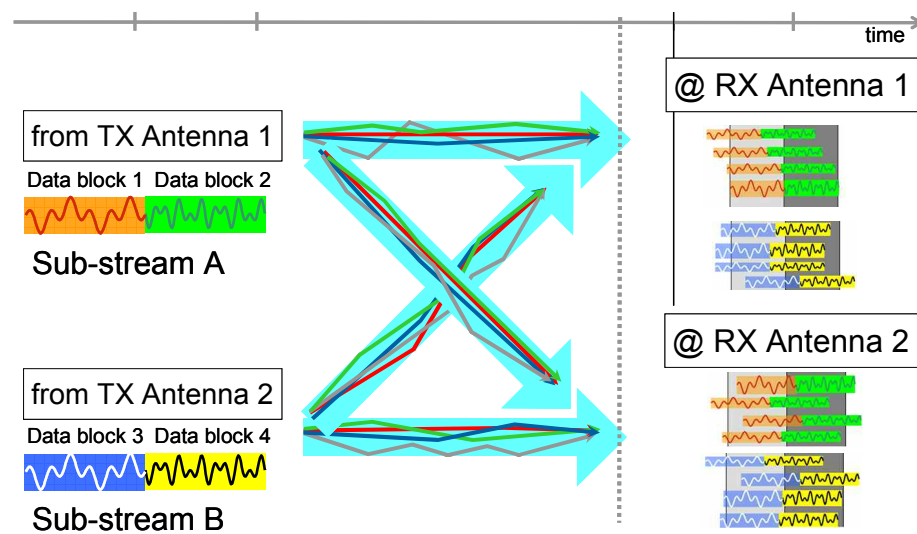


Figure 1: Principle of 2×2 MIMO with 2 parallel downlink data streams

Complex fading scenarios have been derived from real world conditions. In a mandatory test they are used to verify the conducted MIMO performance of a device (see for example LTE specification [4]).

In addition the influence of the antennas on the MIMO performance must be evaluated by radiated measurements.

To simulate the multipath environment with multiple clusters in an anechoic chamber, sophisticated setups are proposed with antenna arrays of eight elements fed by multiple faders (Figure 2). Due to its complexity and incompatibility with existing OTA setups and chambers such a test system requires huge investments.

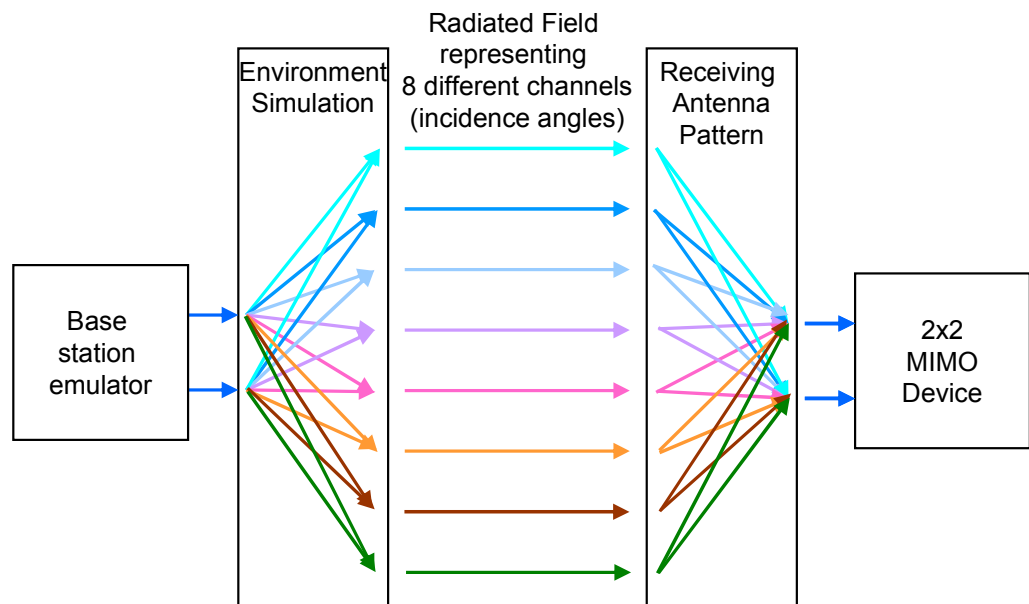


Figure 2: Example for a complex MIMO environment simulation requiring 16 antenna elements and 2x16 fading paths for dual polarized operation

2.2 Split of MIMO measurements

The 2×2 MIMO operation requires uncorrelated data streams at the receiver inputs with sufficient signal-to-noise ratio. Based on uncorrelated data streams at the base station the correlation of the signals at the receiver input is affected on one hand by the fading scenario due to the environment, and on the other hand by the correlation of the receive antennas for the angles of arrival (AoA) and polarizations (Figure 3). A large number of independent channels interfaces with the UE. The receive antennas may respond differently at different spherical angles and field polarizations.

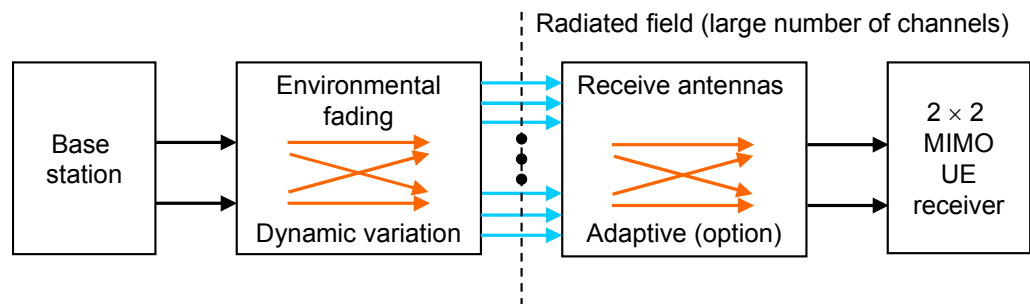


Figure 3: True communication channel determined by environmental fading and receive antennas

For known patterns of the receive antennas the signal coupling can be described as an additional correlation component. This additional component has an impact on the MIMO performance if it increases correlation of the data streams at the receiver inputs of the user equipment (UE). Ideal MIMO antennas would not have an additional influence on the MIMO throughput (TP) at all.

To characterize the overall MIMO performance of a device it has to be tested against different environment scenarios and with different device orientations within each scenario. In real environments there are statistical distributions of angles of arrival and polarizations. To characterize the antenna correlation it is sufficient to use two channels with selected angles of arrival and polarizations. Testing for an appropriate set of such channel parameters allows to describe the radiated characteristics of the receive antennas completely.

The performance of the UE receiver on the other hand is not directly related to the performance of the antenna system. As a consequence we propose to split the test of overall MIMO performance into two separate measurements where the characterized component is marked in yellow (Figure 4 and Figure 5).

The conducted tests are mandatory as part of the 3GPP device certification [4]. These tests aim in verification of the UE receiver when dynamically changing communication channel parameters to represent environmental fading (Figure 4).

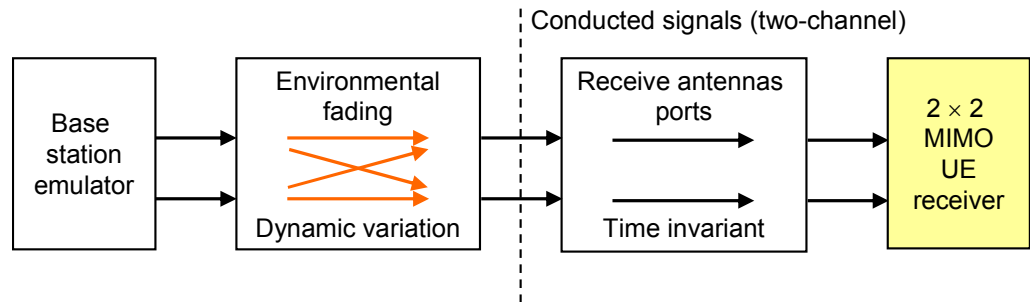


Figure 4: Conducted measurement of MIMO performance with dynamically faded signals

This white paper shows how the OTA measurement can be performed according to the two-channel method using two test antennas (Figure 5). Various angles of arrival and field polarizations are used during the test, whereas effects of user body presence, for example, are selected as static sets of environmental parameters. Furthermore possible adaptive algorithms which control smart receive antennas are also verified by the method.

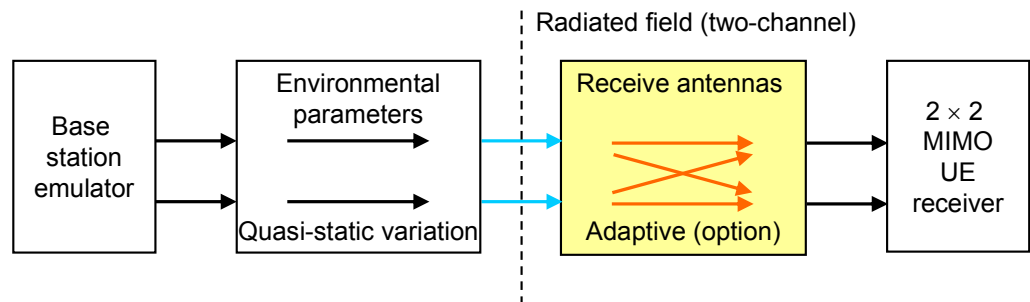


Figure 5: OTA characterization of the receive antennas for representative sets of environmental parameters

The presented OTA method is complementary to the conducted tests. This approach significantly reduces both complexity and costs compared with a setup of a complete multipath propagation scenario.

3 Theoretical Model of the R&S MIMO OTA Test Proposal

3.1 Static MIMO model

In frequency domain, a MIMO transmission is described by the channel matrix \mathbf{H} with $N_R \times N_T$ elements for N_R receiving and N_T transmitting antennas [5]

$$\mathbf{y}(i) = \mathbf{H}\mathbf{x}(i) + \mathbf{n}(i)$$

where the \mathbf{H} matrix is static (constant) for each i -th data sample

$$\mathbf{H} = \begin{bmatrix} h_{11} & h_{12} & \cdots & h_{1N_T} \\ h_{21} & h_{22} & \cdots & h_{2N_T} \\ \vdots & \vdots & \ddots & \vdots \\ h_{N_R 1} & h_{N_R 2} & \cdots & h_{N_R N_T} \end{bmatrix}$$

$\mathbf{x}(i)$ represents a vector of the N_T transmitted i -th data samples of a base station,

$$\mathbf{x}(i) = [x_1(i), \dots, x_{N_T}(i)]^T$$

where T denotes the vector transposition.

$\mathbf{y}(i)$ represents a vector of the N_R data samples received by a user equipment (UE)

$$\mathbf{y}(i) = [y_1(i), \dots, y_{N_R}(i)]^T$$

$\mathbf{n}(i)$ represents a vector of the N_R received noise samples

$$\mathbf{n}(i) = [n_1(i), \dots, n_{N_R}(i)]^T$$

which is an uncorrelated signal mainly related to thermal noise of the UE receiver.

A UE recovers the transmitted signal $\mathbf{x}(i)$ from the received signal $\mathbf{y}(i)$ using the estimate of the channel matrix $\hat{\mathbf{H}}$ superimposed by uncorrelated noise $\mathbf{n}(i)$. In general, recovery of $\mathbf{x}(i)$ is an inverse problem which might be ill-conditioned. Recovery of each data sample $x(i)$ provides the estimate of the true solution $\hat{x}(i)$. The accuracy of the estimate $\hat{x}(i)$ depends on the condition number of the channel matrix estimate $\kappa(\hat{\mathbf{H}})$ and on the ratio of the noise $n(i)$ to the received signal $y(i)$. In other words, the closer the channel matrix is to being a singular matrix, the larger the increase of the estimate error due to the presence of noise will be [5]. The upper bound of the relative estimate error is

$$\frac{|\delta x(i)|}{|x(i)|} \leq \frac{|n(i)|}{|y(i)|} \kappa(\hat{\mathbf{H}})$$

where the estimate error $\delta x(i)$ is the difference between the estimate of the data sample and its true value

$$\delta x(i) = \hat{x}(i) - x(i)$$

and $\kappa(\hat{\mathbf{H}})$ is the ratio between the maximum and minimum singular values of the matrix estimate $\sigma_{\max}(\hat{\mathbf{H}})$, $\sigma_{\min}(\hat{\mathbf{H}})$ respectively. The ratio $\kappa(\hat{\mathbf{H}})$ is always larger or equal one.

$$\kappa(\hat{\mathbf{H}}) = \frac{\sigma_{\max}(\hat{\mathbf{H}})}{\sigma_{\min}(\hat{\mathbf{H}})} \geq 1$$

In order to optimize error-free reception of data samples $\mathbf{x}(i)$, the condition number of the channel matrix estimate $\kappa(\hat{\mathbf{H}})$ and the noise level $\mathbf{n}(i)$ should be kept as low as possible.

3.2 Antenna receiving patterns in static MIMO model

In the following a static model for radio downlink (DL) transmission in MIMO 2×2 mode ($N_R = N_T = 2$) will be presented. The model is shown in Figure 6 and can be easily extended for a higher number of antennas N_R, N_T .

\mathbf{T}_1 and \mathbf{T}_2 are vector angular distributions of the electric field incident on the antennas of the UE created by radiation of base station (BS) signals x_1 and x_2 respectively. The distributions include all propagation paths and are composed of a set of plane waves

$$\begin{aligned} \mathbf{T}_1(\varphi, \theta) &= T_{\varphi 1}(\varphi, \theta) \cdot \hat{\mathbf{a}}_{\varphi} + T_{\theta 1}(\varphi, \theta) \cdot \hat{\mathbf{a}}_{\theta} \\ \mathbf{T}_2(\varphi, \theta) &= T_{\varphi 2}(\varphi, \theta) \cdot \hat{\mathbf{a}}_{\varphi} + T_{\theta 2}(\varphi, \theta) \cdot \hat{\mathbf{a}}_{\theta} \end{aligned}$$

where $\hat{\mathbf{a}}_{\varphi}$ and $\hat{\mathbf{a}}_{\theta}$ are orthogonal unit vectors associated with φ and θ respectively. T_{φ} and T_{θ} represent the two orthogonal linear polarizations of the field vector of the signals \mathbf{T}_1 and \mathbf{T}_2 .

\mathbf{R}_1 and \mathbf{R}_2 are the electric field receiving patterns of the UE antennas defined at the common reference point P and for true UE load impedances. The patterns include possible cross-coupling between antennas and mismatch losses.

$$\begin{aligned} \mathbf{R}_1(\varphi, \theta) &= R_{\varphi 1}(\varphi, \theta) \cdot \hat{\mathbf{a}}_{\varphi} + R_{\theta 1}(\varphi, \theta) \cdot \hat{\mathbf{a}}_{\theta} \\ \mathbf{R}_2(\varphi, \theta) &= R_{\varphi 2}(\varphi, \theta) \cdot \hat{\mathbf{a}}_{\varphi} + R_{\theta 2}(\varphi, \theta) \cdot \hat{\mathbf{a}}_{\theta} \end{aligned}$$

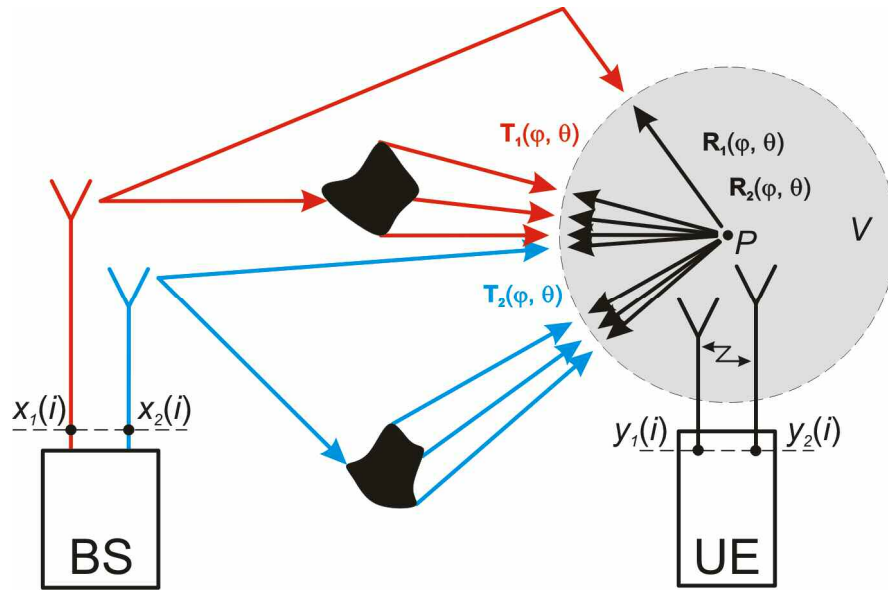


Figure 6: General radio DL transmission in MIMO 2x2 mode

The definition of the received signal at the UE antenna port [6] is extended for two independent incoming fields to represent the MIMO mode. The detected signal y_1 at the UE antenna port is proportional to the dot product of the receiving pattern \mathbf{R}_1 with both incoming field distributions \mathbf{T}_1 and \mathbf{T}_2 integrated over all spherical angles superimposed by noise n_1

$$y_1(i) = c \left(\int_{\varphi=0}^{2\pi} \int_{\theta=0}^{\pi} \mathbf{R}_1(\varphi, \theta) \cdot \mathbf{T}_1(\varphi, \theta) \sin(\theta) d\theta d\varphi \cdot x_1(i) + \int_{\varphi=0}^{2\pi} \int_{\theta=0}^{\pi} \mathbf{R}_1(\varphi, \theta) \cdot \mathbf{T}_2(\varphi, \theta) \sin(\theta) d\theta d\varphi \cdot x_2(i) \right) + n_1(i)$$

where c is a proportionality constant.

Similarly the detected signal y_2 can be noted as

$$y_2(i) = c \left(\int_{\varphi=0}^{2\pi} \int_{\theta=0}^{\pi} \mathbf{R}_2(\varphi, \theta) \cdot \mathbf{T}_1(\varphi, \theta) \sin(\theta) d\theta d\varphi \cdot x_1(i) + \int_{\varphi=0}^{2\pi} \int_{\theta=0}^{\pi} \mathbf{R}_2(\varphi, \theta) \cdot \mathbf{T}_2(\varphi, \theta) \sin(\theta) d\theta d\varphi \cdot x_2(i) \right) + n_2(i)$$

Coupling between BS and UE antennas can be noted in a matrix form

$$\begin{bmatrix} y_1(i) \\ y_2(i) \end{bmatrix} = \begin{bmatrix} h_{11} & h_{12} \\ h_{21} & h_{22} \end{bmatrix} \cdot \begin{bmatrix} x_1(i) \\ x_2(i) \end{bmatrix} + \begin{bmatrix} n_1(i) \\ n_2(i) \end{bmatrix}$$

$$= c \begin{bmatrix} \int_{\varphi=0}^{2\pi} \int_{\theta=0}^{\pi} \mathbf{R}_1(\varphi, \theta) \cdot \mathbf{T}_1(\varphi, \theta) \sin(\theta) d\theta d\varphi & \int_{\varphi=0}^{2\pi} \int_{\theta=0}^{\pi} \mathbf{R}_1(\varphi, \theta) \cdot \mathbf{T}_2(\varphi, \theta) \sin(\theta) d\theta d\varphi \\ \int_{\varphi=0}^{2\pi} \int_{\theta=0}^{\pi} \mathbf{R}_2(\varphi, \theta) \cdot \mathbf{T}_1(\varphi, \theta) \sin(\theta) d\theta d\varphi & \int_{\varphi=0}^{2\pi} \int_{\theta=0}^{\pi} \mathbf{R}_2(\varphi, \theta) \cdot \mathbf{T}_2(\varphi, \theta) \sin(\theta) d\theta d\varphi \end{bmatrix} \cdot \begin{bmatrix} x_1(i) \\ x_2(i) \end{bmatrix} + \begin{bmatrix} n_1(i) \\ n_2(i) \end{bmatrix}$$

The detected signals y_1, y_2 depend on angular distributions of all patterns $\mathbf{R}_1, \mathbf{R}_2, \mathbf{T}_1$ and \mathbf{T}_2 . Normally, the incident fields $\mathbf{T}_1, \mathbf{T}_2$ vary during operation due to relative change of the UE position in relation to the base station and scattering clusters, e.g. during movement of a user along a street canyon. The receiving patterns $\mathbf{R}_1, \mathbf{R}_2$ may also change during operation when a UE is equipped with smart antennas to maximize data throughput and sensitivity.

Such antennas are capable to adapt their receiving patterns depending on environmental parameters, e.g. angles of arrival of the incident fields or antenna detuning by a user body. The static MIMO model is still applicable here since for the given pair of the incident fields $\mathbf{T}_1, \mathbf{T}_2$ and the case of a user interference the receiving patterns $\mathbf{R}_1, \mathbf{R}_2$ stay time-invariant.

The transmitted signals x_1 and x_2 cannot be recovered from the detected signals y_1 and y_2 if determinant of matrix \mathbf{H} equals zero. In this case signals y_1 and y_2 are totally correlated and $\kappa(\mathbf{H}) = \infty$

$$\det \mathbf{H} = h_{11} \cdot h_{22} - h_{21} \cdot h_{12} = 0$$

In summary the design target for a MIMO wireless device providing $\mathbf{R}_1, \mathbf{R}_2$ should be to assure $\kappa(\mathbf{H}) \rightarrow 1$ for a majority of stochastic scenarios of incident fields $\mathbf{T}_1, \mathbf{T}_2$ in real-world environment of the device use.

3.3 The two-channel method

The goal of the method is a characterization of the impact of the UE antenna array on the MIMO performance using a minimum number of data channels. This is achieved by limiting the number of test antennas to the number of BS antennas required for the selected transmission mode. Since MIMO 2×2 mode ($N_T \times N_R$) has the highest attraction at the moment, the proposed test method was named the *two-channel method*.

It is proposed to decompose real-world detection of MIMO signals by the UE by performing a finite set of throughput measurements with various polarizations and single angular directions of \mathbf{T}_{p1} and \mathbf{T}_{q2} . To achieve this we assume that an incoming field from the BS antennas over two arbitrary directions Ω_1, Ω_2 , is linearly polarized in $\hat{\mathbf{a}}_\varphi$ or $\hat{\mathbf{a}}_\theta$, and has unit magnitude.

$$\begin{aligned} \mathbf{T}_{p1}(\varphi, \theta) &= \mathbf{T}_{p1}(\varphi_1, \theta_1) = \mathbf{T}_{p1}(\Omega_1) = \hat{\mathbf{a}}_p \\ \mathbf{T}_{q2}(\varphi, \theta) &= \mathbf{T}_{q2}(\varphi_2, \theta_2) = \mathbf{T}_{q1}(\Omega_2) = \hat{\mathbf{a}}_q \end{aligned}$$

p, q each define one orthogonal linear polarization of the incident field $p, q \in \{\varphi, \theta\}$. Also the cases are included where p and q refer to the same polarization.

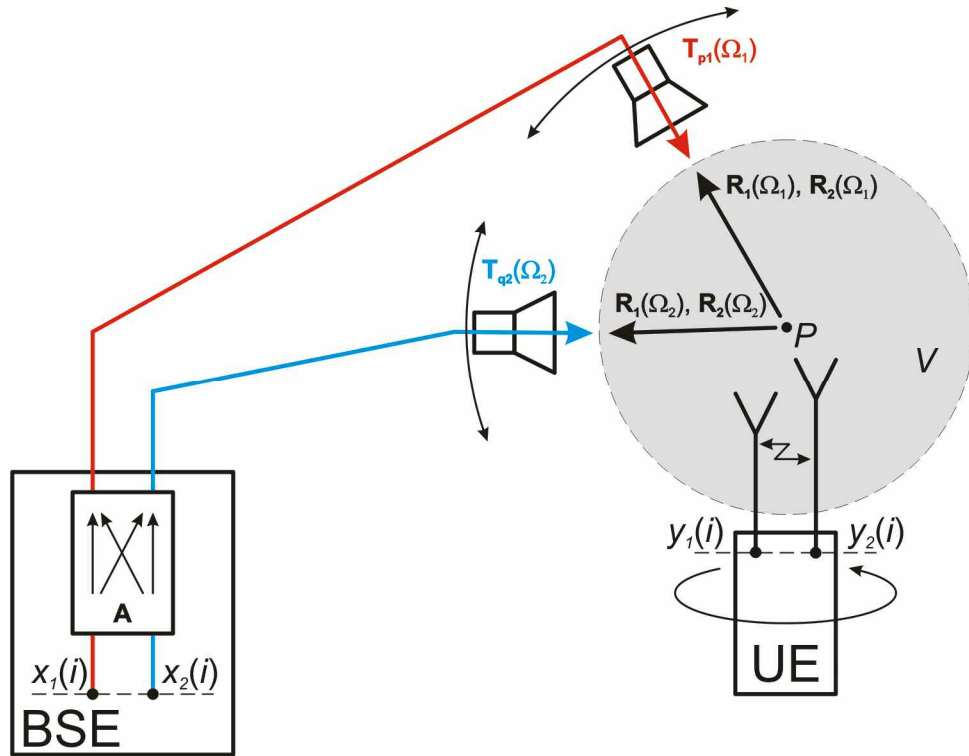


Figure 7: Two-channel method. Static model of DL transmission in MIMO 2×2 mode (incoming signals are linearly polarized and have single AoA)

A general model for such a MIMO OTA approach using the two-channel method is shown in Figure 7 where channel 1 and channel 2 are marked with red and blue color, respectively. The model is noted as

$$\mathbf{y}(i) = \mathbf{H}_{pq}(\Omega_1, \Omega_2) \mathbf{A} \mathbf{x}(i) + \mathbf{n}(i)$$

\mathbf{H}_{pq} denotes four cases of the channel matrix ($\mathbf{H}_{\phi\phi}$, $\mathbf{H}_{\theta\theta}$, $\mathbf{H}_{\phi\theta}$, $\mathbf{H}_{\theta\phi}$) depending on polarization combinations of the incident field \mathbf{T}_{p1} and \mathbf{T}_{q2} .

An auxiliary matrix \mathbf{A} is introduced in order to account for complex transfer functions of two RF channels between the reference plane of a base station emulator (BSE) and the field strength generated by the test antennas at the reference point P . Secondly, the matrix \mathbf{A} allows to control the condition number of the matrix multiplication $\kappa(\mathbf{H}_{pq}\mathbf{A})$. The matrix \mathbf{A} can be controlled by fading settings, for example in the BSE.

$$\mathbf{A} = \begin{bmatrix} a_{11} & a_{12} \\ a_{21} & a_{22} \end{bmatrix}$$

Then $\mathbf{y}(i)$ can be written as

$$\begin{bmatrix} y_1(i) \\ y_2(i) \end{bmatrix} = c \begin{bmatrix} \mathbf{R}_1(\Omega_1) \cdot \mathbf{T}_{p1}(\Omega_1) & \mathbf{R}_1(\Omega_2) \cdot \mathbf{T}_{q2}(\Omega_2) \\ \mathbf{R}_2(\Omega_1) \cdot \mathbf{T}_{p1}(\Omega_1) & \mathbf{R}_2(\Omega_2) \cdot \mathbf{T}_{q2}(\Omega_2) \end{bmatrix} \cdot \begin{bmatrix} a_{11} & a_{12} \\ a_{21} & a_{22} \end{bmatrix} \cdot \begin{bmatrix} x_1(i) \\ x_2(i) \end{bmatrix} + \begin{bmatrix} n_1(i) \\ n_2(i) \end{bmatrix}$$

Four cases of matrix \mathbf{H}_{pq} are due to various combinations of the scalar field components of $R_{p1}, R_{q2}, R_{p2}, R_{q1}$ at directions Ω_1, Ω_2 .

$$\mathbf{H}_{pq}(\Omega_1, \Omega_2) = c \begin{bmatrix} R_{p1}(\Omega_1) & R_{q1}(\Omega_2) \\ R_{p2}(\Omega_1) & R_{q2}(\Omega_2) \end{bmatrix}$$

In order to verify MIMO performance of the UE only as a function of UE receiving patterns the condition number of the auxiliary matrix should be one. In this case $\kappa(\mathbf{H}_{pq}\mathbf{A}) = \kappa(\mathbf{H}_{pq})$. The proportionality constant c does not influence the value of $\kappa(\mathbf{H}_{pq})$. Accordingly, the matrices \mathbf{H}_{pq} define uniquely MIMO receiving characteristics of the tested UE. This is achieved when in the ideal case

$$\mathbf{A} = \begin{bmatrix} \alpha & 0 \\ 0 & \alpha \cdot e^{-j\beta} \end{bmatrix} \Rightarrow \kappa(\mathbf{A}) = 1$$

where α is an arbitrary complex constant describing the path loss of two RF channels between BSE and test antennas. $\beta \in (-\pi, \pi]$ is an arbitrary phase shift describing the difference in electrical length of the two RF channels. Hence it is not necessary to compensate various electrical lengths of the RF channels. This simplifies the calibration procedure of the MIMO OTA test system.

On the contrary, the total path loss of both RF channels must be the same $|a_{11}| = |a_{22}|$ to obtain $\kappa(\mathbf{A}) = 1$. The total path loss is caused by all system components influencing the magnitude of the signal between its generation at the BSE, $x(i)$, and the reference point P , i.e. free space attenuation, absolute gain of test antennas, attenuation of RF cables, switching matrix and the internal components of the BSE.

In a real-world environment, the magnitudes of the incident fields on the UE at the point P due to data streams x_1, x_2 are not equal, i.e. $|a_{11}| \neq |a_{22}|$, and the combined data streams may impinge on the UE from the same angle of arrival, i.e. $|a_{12}| \neq 0, |a_{21}| \neq 0$. In this case $\kappa(\mathbf{A}) > 1$ which leads to a reduced sensitivity of the UE. The constraint $\kappa(\mathbf{A}) = 1$ was proposed to assure uniqueness of the results for the two-channel method.

4 Test plan for MIMO OTA measurements

4.1 Test case definition

Performance tests over the air (OTA) target mainly on the UE antenna properties. Such tests have to evaluate parameters which cannot be tested in conducted testing.

This test plan describes assessments of multiple antennas on user equipment (UE) terminals used for multiple-input multiple-output (MIMO) transmissions. For the moment tests are only specified for downlink 2×2 MIMO operation. In these measurements the MIMO antenna characteristics have to be evaluated for various possible angles of arrival.

Good MIMO operation of a UE is assured when the receiving antennas are well decoupled. Only then the data streams can be fully recovered. This is a prerequisite for high data rates and stable receive conditions.

The selection of test cases is guided by the following principles:

1. OTA test cases are to focus on the physical UE implementation aspects which *have to* be characterized in an OTA test environment. Conducted tests complete the UE verification.
2. Including fading by using channel models blurs the measurement results and makes it difficult to clearly identify the UE's antenna performance.
3. Each test case should be kept as simple as possible and must assure reproducibility with accurate calibration.
4. Test setups which allow reusing existing OTA chambers are much preferred.

It is sufficient to characterize MIMO performance with just two OTA test cases. These two test cases are referred to in the following sections as:

- a. Noise-limited performance in transmit diversity mode using a robust QPSK modulation
- b. Peak performance in spatial multiplexing mode with a 64QAM modulation of high spectral efficiency

4.2 Noise-limited OTA performance in transmit diversity mode

4.2.1 Goal of the test case

Downlink Transmit Diversity (TD) is a rather important transmission mode in LTE when being close to the cell edge. This mode provides fair reliability of the link and of throughput without knowledge of channel at the transmitter side. The same data stream is transmitted twice, using different coding (e.g. Alamouti space-time block code). This increases the probability for the UE to successfully decode the information.

By selecting a very robust modulation of QPSK, the receiver sensitivity is pushed to the limits.

The appropriate test case characterizes the UE sensitivity and covers the following physical implementation aspects:

- antenna efficiency
- receiver noise figure
- self-interference
- antenna correlation

4.2.2 Settings for signal routing and the eNodeB emulator

Two output ports of the MIMO eNodeB emulator are connected directly to the ports for the two polarizations of the test antenna. In the TD scheme, two orthogonal signals are routed to the two polarizations of the test antenna simultaneously. Both signals are attenuated asymmetrically to compensate for unequal RF path losses in order to provide equal power at the UE location. P_{iso} is the total output power density of an ideal isotropic radiator placed at the UE location when it is illuminated by both test signals. The test antenna is moved around the unit sphere in a defined grid in order to access all relevant AoAs.

The power P_{iso} is given in terms of RS EPRE, which is the energy per resource element (EPRE) of the reference signal (RS) and is expressed in dBm / 15 kHz. Be aware that reference signals occur at different points in time on each port.

eNodeB settings for noise-limited test case			
LTE mode			
DL MIMO mode	Transmit Diversity (TD)		
Schedule type	User-defined channel		
Downlink settings		Uplink settings	
Cell bandwidth	10 MHz	Cell bandwidth	10 MHz
Number of RB	50	Number of RB	50
Start RB	0	Start RB	0
Modulation	QPSK	Modulation	QPSK
TBS Idx / value	0	TBS Idx / value	0
MCS index	0	MCS index	0
Maximum throughput for one channel	1384 kbit/s	Maximum throughput for one channel	1384 kbit/s
Maximum throughput for both channels	1384 kbit/s	Transmit power control	closed loop, target power = -10 dBm
Maximum number of HARQ transmissions	1		
PDSCH power offset relative to RS EPRE [dB]	$\rho_A = -3$ $\rho_B = -3$		
AWGN	OFF		
P_{iso} DL power	RS EPRE in dBm / 15 kHz		
Determining the figure of merit			
Number of subframes for BLER evaluation	2000		
Error rate threshold	10 %		

Table 1: Common TD communication parameters of eNodeB emulator

4.2.3 Sensitivity threshold search

The sensitivity threshold search decreases DL power while observing the BLER. Since the break-off of the connection occurs rather rapidly, the step size for this search has to be adjusted to the technology. In many cases a step size of the order of 2 dB will possibly change the reported BLER from 0 % to 100 %. In such cases the step size should not be larger than 0.5 dB.

On the other hand, due to the antenna pattern and possible effects of phantoms, it is not unusual to observe a change in sensitivity of the order of several dB. This means that the starting power for the sensitivity threshold search has to be high enough to ensure a stable link, even when changing the geometrical constellation.

In order to optimize the search process it is advisable to start the search with bigger steps, e.g. 2 dB, and once reaching the area where the BLER deviates from 0 %, a finer stepping has to be used, possibly searching on either side of the power level with respect to the currently used power. Using fewer frames during the coarse steps will speed up the measurement, but will also result in a larger uncertainty of the BLER value obtained. The number of frames indicated in Table 1 is the one which has to be applied during the fine step search.

Once two power levels have been found, one with a BLER larger than the threshold BLER, and one smaller, a linear interpolation between both power levels gives the effective isotropic sensitivity value *EIS*, i.e. the power level at which the UE is assumed to deliver a BLER equaling the threshold value.

4.2.4 Measurement at single geometrical constellation

Before moving the test antenna and the UE to a given geometrical constellation, a connection between eNodeB emulator and UE has to be established. This may require manual operation.

For each orientation of the test antenna and of the UE, a downlink sensitivity measurement is done. The measurement starts from a high power value. The power level then is decreased until the error rate increases above the level given in the appropriate table above. The power level is recorded as sensitivity threshold *EIS* as described in 4.2.3.

In case of a lost connection, up to two reconnection requests will be issued. If a connection cannot be established, the measurement will be recorded as having an *EIS* of the highest power level used in the test.

4.2.5 Variation of geometrical constellations

Repeat this measurement *M* times by rotation of test antenna and / or UE until the unit sphere is sampled by a predefined resolution.

Geometrical constellations		
Parameter	Value	Description
φ	0°, 30°, ..., 330°	azimuth position (total of 12)
θ	30°, 60°, ..., 150°	elevation position (total of 5) of test antenna
<i>M</i>	60 × 1 = 60	Spatial constellations times polarization combinations

Table 2: Constellations for TD test

4.2.6 Evaluation of the figure of merit

The figure of merit (FOM) to be reported is the Cumulative Distribution Function (CDF) of the sensitivity S over the set $\hat{\Omega}$ of measured AoAs:

$$\text{CDF}_S(S; \hat{\Omega}; \text{FRC}, \text{BLER}) = \text{Prob}\{P_{iso} \leq S\}.$$

FRC refers to the fixed reference channel described in Table 1, and BLER is the threshold percentage given in the same table. The CDF curve describes the probability that the equivalent isotropic power (per resource element) P_{iso} which is required to maintain a BLER below the specified threshold will not exceed S for an arbitrary AoA.

4.2.7 Using CSI information

An alternative approach for LTE UEs is based on the channel state information (CSI) feedback from the UE. The following quantities are available:

- Channel quality indicator (CQI)
- Rank indicator (RI)
- Precoding matrix indicator (PMI)

For the moment this test plan is going to use CQI information only. The test using CSI will be performed in the following way:

The eNodeB emulator is requesting the CQI information for each constellation using a pre-defined starting DL power level. The power level then is decreased and the UE requested for CQI reporting until a change in the reported CQI value is crossing from one condition to the next, namely from $\text{CQI} \geq 7$ to $\text{CQI} \leq 6$. This corresponds to the preferred modulation changing from 16QAM to QPSK. The value for the first power level where the CSI has changed is recorded and will be named $P_{CS}(i)$ for the i^{th} constellation.

This is repeated for all constellations. At the end, the antenna is positioned to the constellation with the lowest power recorded, $P_{CS}(i_{min})$. This constellation is having the best sensitivity. At this constellation then a power sweep is made using not only the power levels covered during the test at different constellations, but also extending to lower power levels according to the regular sensitivity threshold search. The power level at which the sensitivity threshold is reached, evaluated according to section 4.2.3, is named $EIS(i_{min})$.

The recorded power levels have then to be scaled in the following way:

$$EIS(i) = P_{CS}(i) + EIS(i_{min}) - P_{CS}(i_{min}).$$

4.3 Peak performance measurements in spatial multiplexing mode

4.3.1 Goal of the test case

Another aspect of MIMO performance is the device's capability to benefit from multipath propagation. The peak data rate is achieved when an optimal channel is given, using spatial multiplexing mode.

In the spatial multiplexing (SM) case the BS antennas transmit orthogonal data in two separate streams, each using a dedicated antenna (or polarization). Filling both streams with different data thus increases data rates by a factor of two when using 2×2 SM MIMO.

This measurement is aimed to evaluate whether the antenna system is able to meet the UE's performance target including the following physical properties:

- spatial / polarization diversity
- gain imbalance
- antenna correlation
- MIMO detector performance (to some extent)

The Open Loop Spatial Multiplexing (OLSM) MIMO mode together with a rather complex modulation of 64QAM allows the highest throughput values.

4.3.2 Settings for signal routing and the eNodeB emulator

In this setup, the two output ports of the eNodeB emulator are connected to the ports of the corresponding polarization of each of the two test antennas (horizontal and vertical). Since each test antenna is dual polarized, there are in total four combinations of polarizations to be measured: $\varphi - \varphi$, $\theta - \theta$, $\varphi - \theta$, $\theta - \varphi$.

The downlink power level P_{iso} is defined as the output power of the two output ports of the eNodeB emulator. Correction factors have to be applied independently to both ports depending on the frequency and on the chosen path to the test antenna. Each downlink power from the eNodeB emulator to the UE shall have the same level at the UE.

The power P_{iso} is given in terms of RS EPRE, which is the energy per resource element (EPRE) of the reference signal (RS) and is expressed in dBm / 15 kHz.

eNodeB settings for peak performance test case			
LTE mode			
DL MIMO mode	2 × 2 Open Loop Spatial Multiplexing (OLSM)		
Schedule type	User-defined channel		
Downlink settings		Uplink settings	
Cell bandwidth	10 MHz	Cell bandwidth	10 MHz
Number of RB	50	Number of RB	50
Start RB	0	Start RB	0
Modulation	64QAM	Modulation	16QAM
TBS Idx / value	24	TBS Idx / value	19
MCS index	26	MCS index	20
Maximum throughput for one channel	30576 kbit/s	Maximum throughput for one channel	21384 kbit/s
Maximum throughput for both channels	61152 kbit/s	Transmit power control	closed loop, target power = -10 dBm
Maximum number of HARQ transmissions	4		
PDSCH power offset relative to RS EPRE [dB]	$\rho_A = -3$ $\rho_B = -3$		
AWGN	OFF		
P_{iso} DL power	RS EPRE in dBm / 15 kHz		
Determining the figure of merit			
Number of subframes for TP evaluation	2000		

Table 3: Common OLSM communication parameters of eNodeB emulator

4.3.3 Measurement at single geometrical constellation

Before moving the test antennas and the UE to a given geometrical constellation, a connection between eNodeB emulator and UE has to be established.

For each orientation of the test antenna and of the UE, a throughput measurement is made using the same power level P_{iso} . If no connection can be established, the corresponding TP value is assumed to be 0. Four polarization combinations are measured at each geometrical constellation.

4.3.4 Variation of geometrical constellations

In order to sample all areas of the unit sphere around the UE, and at the same time varying separation between the AoAs of the two antennas, the following constellations as given in Table 4 are required.

Geometrical constellations		
Parameter	Value	Description
φ	0°, 30°, 60°, ..., 150°	azimuth position (total of 6)
$\theta_1 = \theta_2$	15°, 45°, 75°, ..., 165°	elevation position (total of 6) of test antennas
M	$36 \times 4 = 144$	Spatial constellations times polarization combinations

Table 4: Constellations for OLSM test

The value of φ rotating the UE defines the plane in which the test antennas move. The value of θ is the same for both antennas. This means that each antenna is moving along the opposite semi-circle with respect to the vertical axis of the UE. When θ increases from 15° to 75°, also the offset between both antennas increases from 30° to 150°. When θ increases further from 105° to 165°, the offset between both antennas decreases from 150° to 30°.

4.3.5 Evaluation of the figure of merit

The metric to be reported is the Complementary Cumulative Distribution Function (CCDF) of throughput TP :

$$\text{CCDF}_{TP}(t; C, \text{FRC}, P_{\text{iso}}) = 1 - \text{Prob}\{TP < t\}$$

C denotes the set of applied constellations and t is a given throughput threshold. The CCDF curve shall have the horizontal axis from 0 % to 100 % relative TP , and the vertical axis as probability ranging from 0 % to 100 %. The CCDF curve shows the probability (vertical axis), with a given DL power at the UE's position, of having a throughput *not* falling below each performance threshold (horizontal axis) with a given FRC and for the most common usage scenarios.

A weighting function for each constellation can be applied in order to compensate geometrical effects or to give special attention to some geometrical constellations.

5 Test site characteristics and UE setup

5.1 UE coordinate system

The following figure is a sketch of the test site with the UE attached to a phantom head. The coordinate system of the UE, xyz , is shown as well as the angles θ and φ . θ ranges from 0° (top) to 180° (bottom). $\varphi = 0^\circ$ is in the orientation of the $+x$ axis, increasing to 90° along the $+y$ axis.

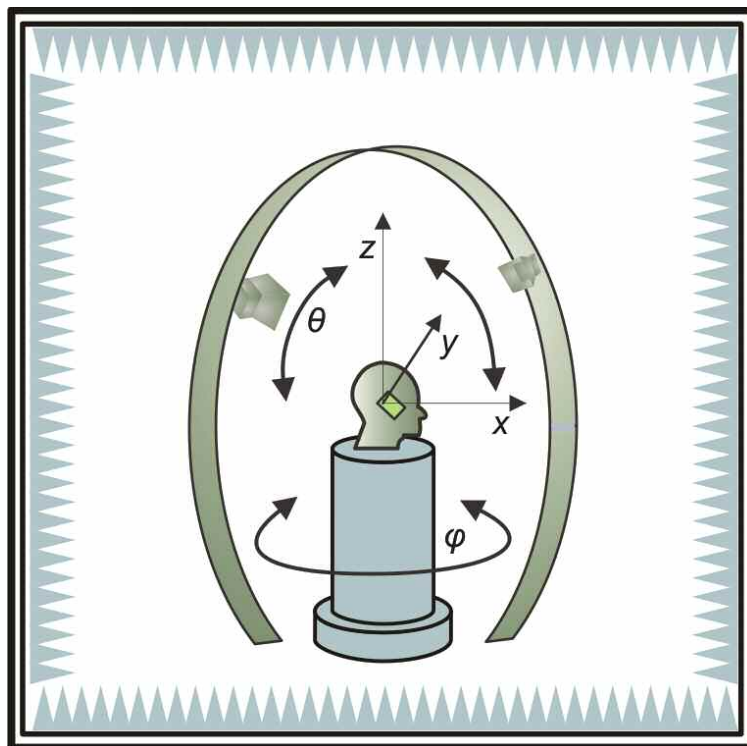


Figure 8: UE coordinate system with antennas in vertical plane

5.2 Set-up with antennas in a vertical plane

An approach for a set-up for antennas in a vertical plane is using moving arms on which the test antennas are attached.

For the azimuth angles, the UE is positioned on a turn table in the center axis of the chamber.

The elevation setting consists of two arms with one dual polarized test antenna on each, which can be rotated around a horizontal axis. In order to have both test antennas in the same plane, the easiest implementation is using one motor drive with one antenna arm on one side of the chamber, for example the left side, and another one on the opposite (right) side. With appropriate controls each antenna can be rotated individually to its own elevation angle. RF switches allow the correct routing of the signals.

The distance to the center of the UE's coordinate system is the same for both test antennas.

Another possibility for an implementation of AoAs from the vertical plane is an array of test antennas, all arranged with equal spacing in a vertical plane around the UE's position on the turntable. In order to select any wanted AoA, the corresponding path to the test antenna has to be selected.

Chambers suited for SISO testing and using any of the two approaches are easily converted into a chamber for MIMO testing.

5.3 Set-up with antennas in a horizontal plane

The arrangement for tests with two test antennas in a horizontal plane again is similar to a SISO great circle cut (combined axes) chamber. The UE is mounted on a two-axes positioner, and the test antennas can take arbitrary angles with respect to the UE, but remain in the horizontal plane. The distance to the center of the UE's coordinate system is the same for both test antennas.

It is up to the system layout if the positions of the test antennas are changed manually, by moving a tripod with the test antenna on it, for example, or automatically with some motor drive which relocates the test antenna. As a third possibility one can realize such a system by arranging several test antennas around the UE and switching the signals to the appropriate antennas.

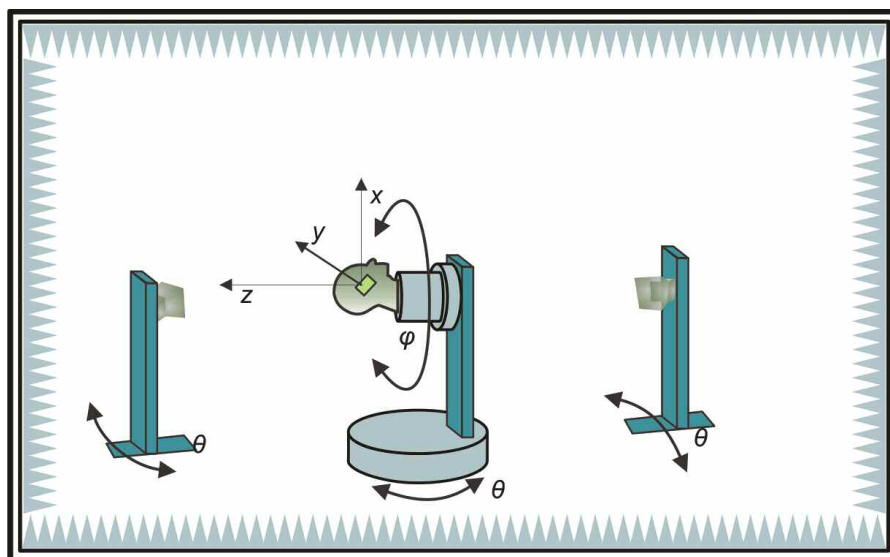


Figure 9: UE coordinate system with antennas in horizontal plane

5.4 Calibration of the test set-up

In order to know exactly the DL level from each of the test antennas, it is required to perform a system calibration. When injecting a known CW signal to one of the test antennas and measuring with a reference antenna with known gain at the UE's position, one can calculate the required correction factor consisting of the cable loss from the generator to the test antenna, the gain of the test antenna, and the free space attenuation between test antenna and reference antenna. This correction factor has to be recorded as a function of frequency. During the measurement the appropriate correction then has to be added to the signal level at the BSE output in order to give the power reaching the UE.

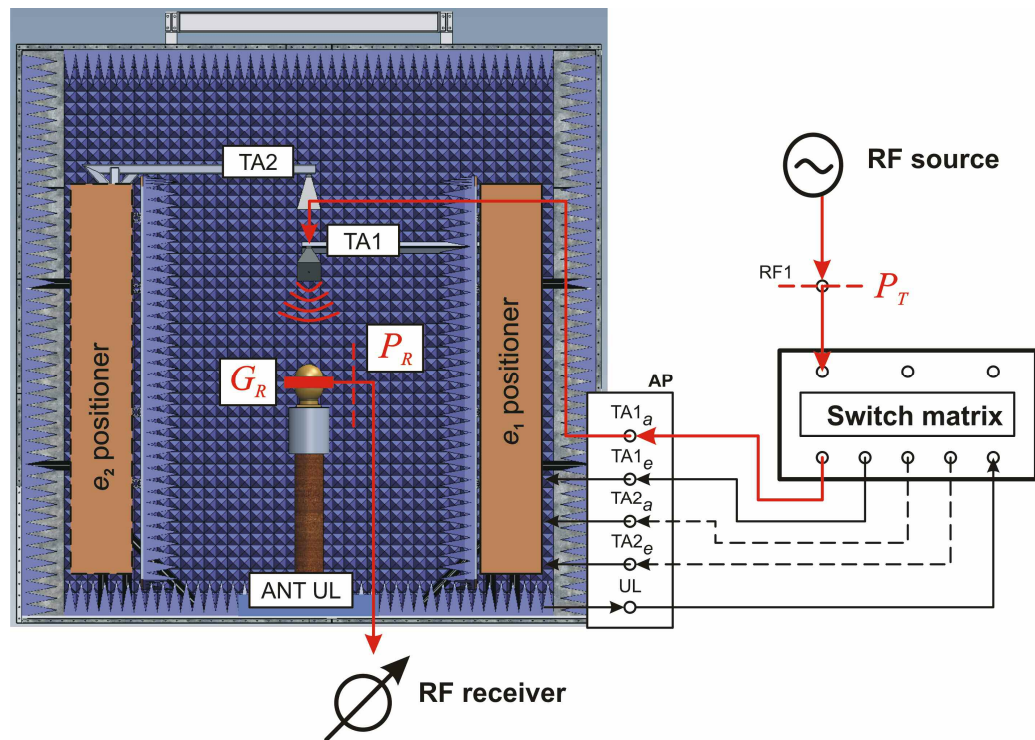


Figure 10: Calibration set-up of TS8991 MIMO OTA test system

$$pathloss = G_R + P_R - P_T$$

G_R : gain of receiving test antenna

P_R : received power at UE reference plane

P_T : transmitted power at eNodeB reference plane

Individual calibration curves have to be recorded for each test antenna and each polarization.

5.5 UE set-up

5.5.1 General considerations and phantoms

For USB-connected modems, the tests shall be made with a host notebook. For embedded modems the notebook itself is the UE. No table or lap phantom is going to be used.

If the UE is a datacard or USB dongle, it shall be tested using a reference notebook. Devices that connect to a USB port shall be connected directly to a USB port on the left or rear side of the notebook. Additional USB cables shall not be used to connect the device to the notebook.

Handheld devices which support voice communication will be tested using a head and hand phantom. Other small form factor devices shall be tested in a free space configuration.

5.5.2 Operation condition of the notebook

The notebook shall be operated in the following configuration when testing USB dongles:

- Transmitting radios
 - WWAN: on
 - All other embedded transmitting radios that are not being tested: off
- Power Management Settings
 - Screensaver: none
 - Turn Off Display: never
 - Turn Off Hard Drive: never
 - System Hibernate: never
 - System Standby: never
- Display (LCD) Backlight: Medium intensity (50% or equivalent)
 - Ambient light sensor: disabled
- Keyboard Backlight: off
- Powered by battery (standard battery only)
- Dynamic control of CPU and clock frequencies: disabled, if possible

The center of the coordinate system is the geometrical center of the notebook with the UE's physical shape neglected.

Testing notebooks with embedded antennas shall be configured similarly.

6 MIMO OTA System Implementation

6.1 System overview

The TS8991 MIMO OTA test system supporting the two-channel method is shown in the block diagram of Figure 11. An OTA chamber contains three angular positioners to control φ , θ_1 , θ_2 angles, two test antennas ANT DL1, ANT DL2 and one communication antenna ANT UL. Furthermore the access panel AP permits five RF connections to the test antennas placed in the chamber. External instrumentation includes the R&S CMW500 wideband radio communication tester and the R&S OSP130 open switch and control platform as a switch matrix. The MIMO OTA test system was built at Rohde & Schwarz according to the diagram shown.

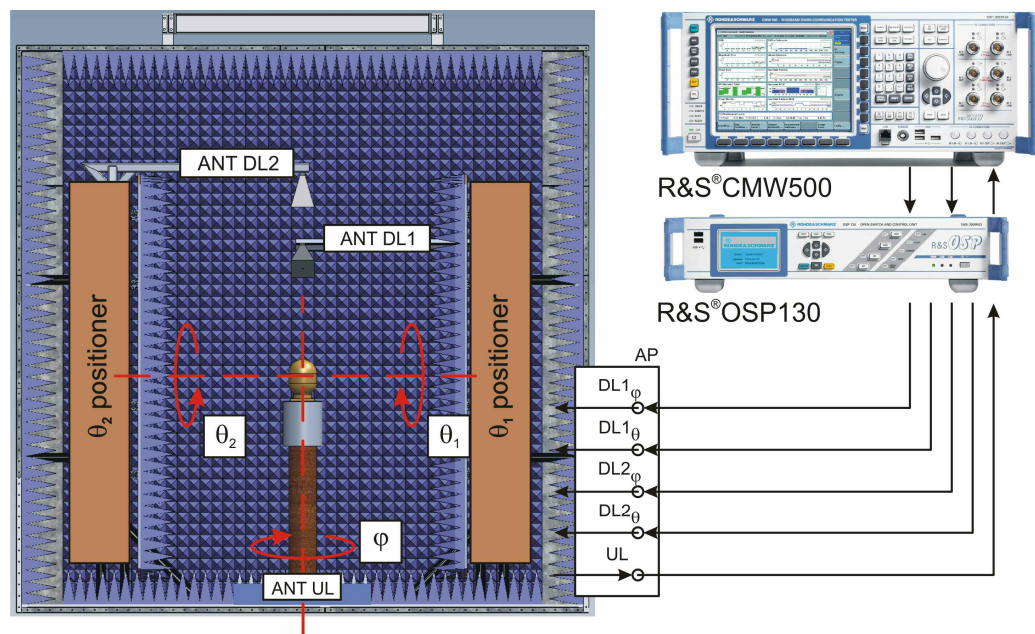


Figure 11: Block diagram of TS8991 MIMO OTA test system supporting two-channel method

6.2 OTA test chamber with internal components

The OTA test chamber with dimensions $5\text{ m} \times 5\text{ m} \times 5\text{ m}$ is lined with pyramid absorbers to provide a shielded anechoic environment for RF measurements. The chamber shown in Figure 12 contains three positioners. Two independent elevation positioners are hidden behind anechoic walls. They control θ_1 , θ_2 angular positions of the test antennas in a φ -plane. A UE is mounted on the top of the azimuth positioner which controls the φ position.

The inclination positioner was not implemented for these tests. All three positioners permit to setup an arbitrary pair of angles of arrival Ω_1 , Ω_2 to illuminate the UE with test fields $\mathbf{T}_{p1}(\Omega_1)$, $\mathbf{T}_{q2}(\Omega_2)$.

Two quad-ridged horn antennas are utilized as test antennas ANT DL1, ANT DL2. Each antenna is capable to create φ or θ orthogonal components of linearly polarized field through the dedicated φ and θ antenna connectors. The test antennas provide the downlink connection to the UE. The circularly polarized communication antenna ANT UL provides the uplink connection to the BSE. The antenna ANT UL is integrated inside the azimuth positioner. All five antenna ports are connected with RF cabling to the external instrumentation through RF connectors (DL1 $_{\varphi}$, DL1 $_{\theta}$, DL2 $_{\varphi}$, DL2 $_{\theta}$, UL) mounted on the access panel (AP).

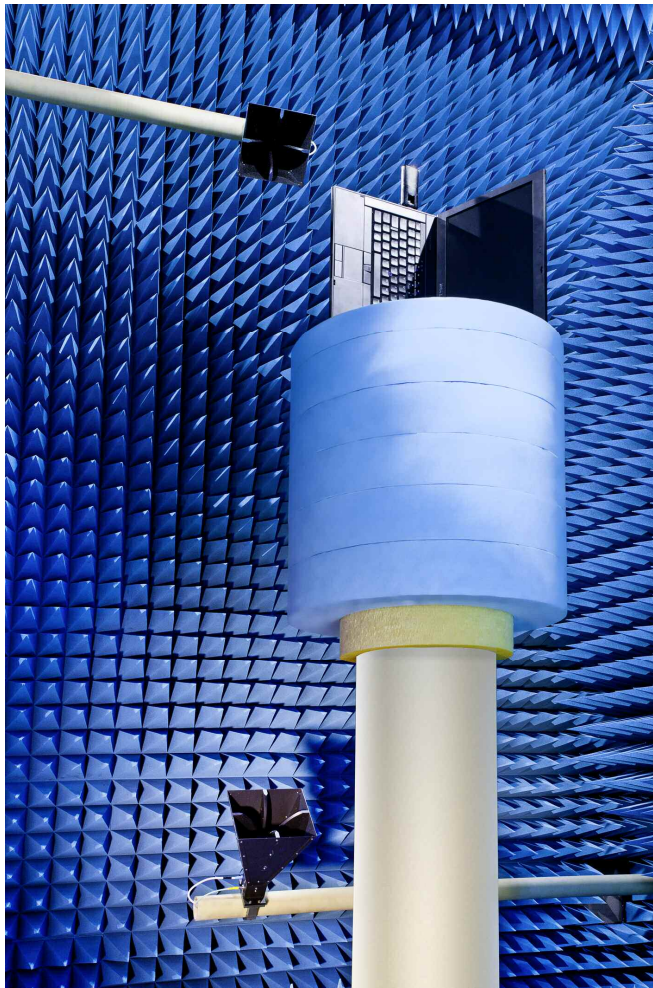


Figure 12: Fully anechoic chamber for MIMO OTA measurements

6.3 External system components

The Wideband Radio Communication Tester R&S CMW500 is utilized as a base station emulator with LTE signaling functionality. In a configuration with two RF frontends it can carry two independent LTE downlink data streams x_1 and x_2 when set to spatial diversity mode. Another RF port receives the LTE uplink signal.

The Open System Platform R&S OSP130 is utilized as a switching matrix to route all the RF signals to adequate ports of the communication and test antennas. An integrated limiting amplifier in the uplink path supports a stable call connection between the UE and the BSE when rotating the azimuth positioner.

The whole system is controlled with the R&S AMS32 OTA system software to automate the measurement procedure and to report measurement results.

The system can be extended to include a fading simulator to verify UE performance with an arbitrary and dynamically changing channel matrix \mathbf{H} .

7 Measurement Results

7.1 Summary of 3GPP round robin test with LTE devices

In the RAN4 LTE round robin test evaluating different proposed test methods for testing MIMO OTA performance of LTE devices, Rohde & Schwarz has participated with the test system described in section 5 and has presented results in several contributions ([7], [8], [9], [10], [11]).

Figure 13 shows an example of a CCDF evaluation of six different LTE devices.

The UEs have been measured in OLSM mode at a power level of -100 dBm/15 kHz. This example used a set of constellations different from the proposed ones in Table 3. The CCDF curve clearly tells how many measurement cases out of the total constellation / polarization combinations have higher throughput than the value shown on the horizontal axis. Operators can specify an acceptance criterion in terms of relative throughput percentage and CCDF. For instance, if one requires devices to achieve 75 % of relative throughput in 65 % of the constellations, the criterion is represented as a 75 % \times 65 % rectangular box. Only devices with the CCDF curve outside of the box (e.g. UE1 and UE2 in Figure 13 would fulfill the criterion).

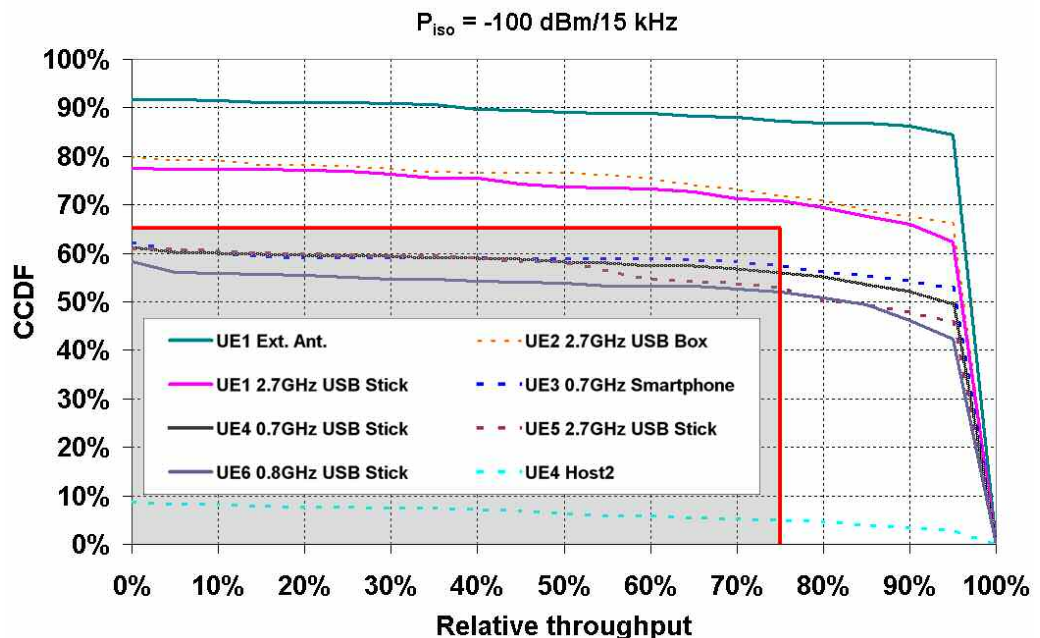


Figure 13: CCDF results for a 3D constellation set from RR test made in OLSM transmission scheme where 100% TP = 23288 kbit/s (MCS index=14)

7.2 Noise-limited performance in transmit diversity mode

7.2.1 Example of LTE Transmit diversity measurement result

Illustration of CDF statistical metrics is given in Figure 14. The smartphone UE3 (LTE, 0,7 GHz) was operated in transmit diversity mode with MCS index = 0 (QPSK modulation) to achieve the maximum receiver sensitivity. The Probability Distribution Function (PDF) was calculated for 60 measurement constellations according to Table 1. The CDF curve is generated on the PDF over receiver sensitivity. A quality criterion can be easily defined, e.g. for a threshold of -126 dBm/15 kHz more than 50 % of the measurements shall have a better sensitivity.

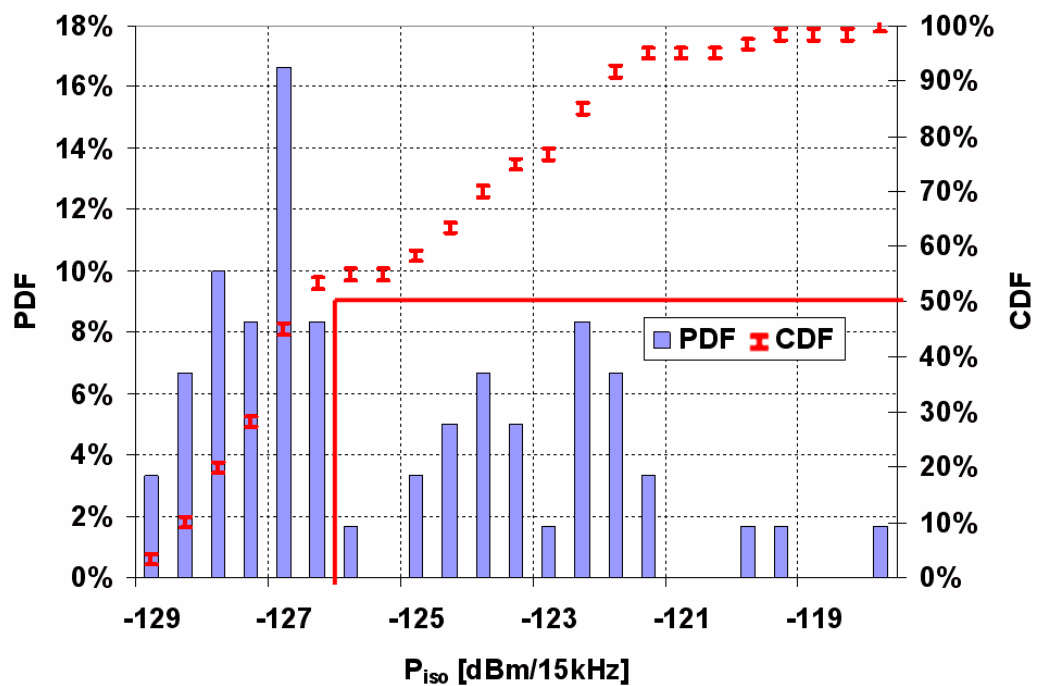


Figure 14: Probability (PDF) and cumulative (CDF) distribution functions of UE3 radiated sensitivity over the set of 60 antenna AoAs

7.3 Peak performance measurements in spatial multiplexing mode

7.3.1 Example of OL spatial multiplexing measurement result

Dependence of DL throughput on various polarization cases of incident test fields is presented in Figure 15 for the smartphone UE3. Selection of antenna geometrical constellations agrees with the set provided in Table 3. 64QAM modulation and high coding rate was selected for both streams to verify peak performance of UE3. Geometrical constellations according to Table 4 were used.

The highest probability of high relative throughput $TP < 81\%$ is obtained when the incident fields carrying uncorrelated data streams are cross-polarized. Then CCDF amounts to 81% for phi-theta and 75% for theta-phi polarized fields. On the other hand UE3 does not provide any throughput when both incident fields are phi polarized at all geometrical constellations of test antennas.

These results suggest that UE3 is equipped with two receiving antennas characterized by good polarization diversity and poor spatial diversity for phi polarized fields. Poor spatial diversity agrees with expectations since the largest dimension of UE3 is approximately 0.3λ at the DL frequency.

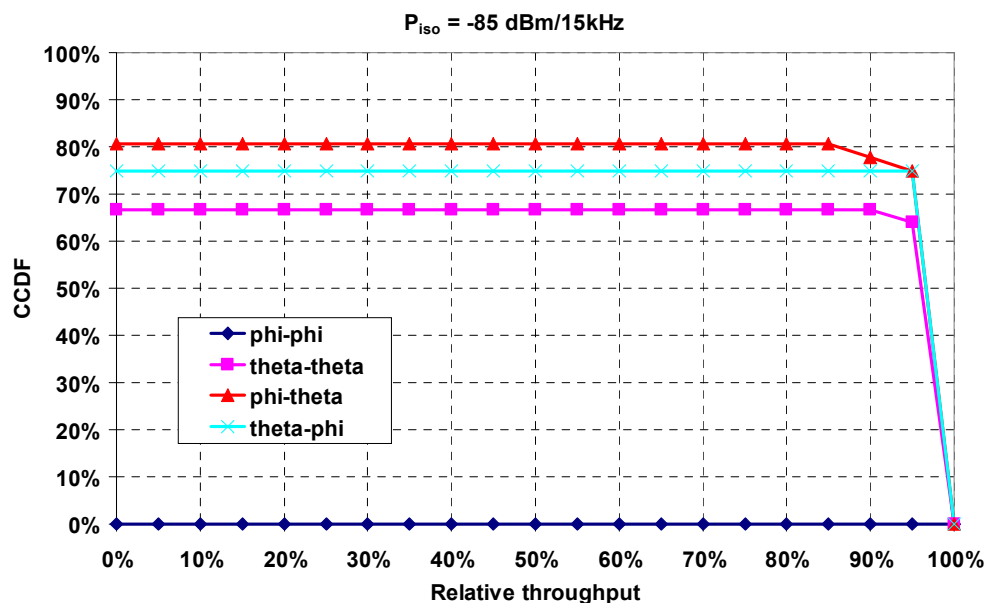


Figure 15: CCDF of UE3 radiated throughput for four polarization cases of test field where 100% TP = 61152 kbit/s (MCS index = 26)

8 Conclusions

Theoretical background was presented for a new simple OTA method to quantify uniquely the sensitivity of MIMO-enabled wireless devices. The two-channel method is based on a static channel model of electromagnetic field coupling between a base station and some user equipment. The method characterizes primarily the influence of the multiple antenna design of the UE on its radiated sensitivity. Thus it is complementary to the verification tests performed in conducted mode which include dynamic channel models [4]. Receiver properties that are not related to the spatial properties of the UE antenna system are to be addressed separately by conducted measurements with identical basic settings of the eNodeB emulator.

The MIMO OTA test plan presented here using the two-channel method for device characterization comprises two types of test cases:

- a) sensitivity measurements in a noise-limited scenario, and
- b) peak performance measurements in a MIMO-favorable channel.

In the first case, the metric to be reported is the CDF of sensitivity using a transmit diversity downlink signal coming from the same AoA but with orthogonal polarization. The CDF relates to outage probability in an arbitrary propagation scenario.

The second test case makes use of two test antennas transmitting signals in open-loop spatial multiplexing mode. The metric to be reported is the CCDF of throughput at some fixed downlink power. It relates to the probability of *not* falling below a given throughput threshold.

The two-channel method might be easily implemented in existing distributed axes OTA test systems for SISO wireless devices. Another angular positioner with a second test antenna needs to be added.

The verification also includes performance of UE smart antennas with adaptive receiving characteristics and load impedances. True load impedance of EUT antennas is assured since the method does not require connecting any auxiliary RF cabling to the antenna ports during the test.

The presented test approach facilitates a systematic OTA verification of MIMO-enabled devices. “Good” or “worse” designs can be distinguished by quantitative and reproducible measurements.

9 Abbreviations

AoA	Angle of arrival (at UE antenna)
AP	Access panel
BLER	Block error rate
BS	Base station
BSE	Base station emulator, like R&S CMW500, R&S CMU200
CDF	Cumulative distribution function
CCDF	Complementary cumulative distribution function
CQI	Channel quality indicator
CSI	Channel state information
DL	Downlink
EIS	Effective isotropic sensitivity (single geometrical point)
eNodeB	Evolved NodeB, LTE base station
EPRE	Energy per resource element
FOM	Figure of merit
FRC	Fixed reference channel
MCS	Modulation coding scheme
MIMO	Multiple input, multiple output
OLSM	Open loop spatial multiplexing
OTA	Over-the-air
PDF	Probability distribution function
PMI	Precoding matrix indicator
RI	Rank indicator
RS	Reference signal
SISO	Single input, single output
SM	Spatial multiplexing
TD	Transmit diversity
TIS	Total isotropic sensitivity
TP	Throughput
TRP	Total radiated power
UE	User equipment = wireless device = mobile phone / modem / notebook
UL	Uplink
WWAN	Wireless Wide Area Network (e.g. GPRS, HSPA)

10 References

- [1] CTIA; Test Plan for Mobile Station Over the Air Performance, Revision 3.0; 2009-04
- [2] 3GPP R4-091710; Rohde & Schwarz; Cost-Effective Over-The-Air Performance Measurements on MIMO Devices; San Francisco, http://ftp.3gpp.org/tsg_ran/WG4_Radio/, 2009-05
- [3] 3GPP R4-104283; Rohde & Schwarz; Two-Channel Method for Evaluation of MIMO OTA Performance of Wireless Devices; Jacksonville, http://ftp.3gpp.org/tsg_ran/WG4_Radio/, 2010-11
- [4] Test specification 3 GPP TS36.521-1 V8.6.0, "User Equipment (UE) conformance specification, Radio transmission and reception, Part 1: Conformance Testing", <http://www.3gpp.org/ftp/Specs/>, 2010-06
- [5] E. Dahlman, S. Parkvall, J. Sköld, P. Beming, 3G Evolution: HSPA and LTE for Mobile Broadband, 2nd ed., Oxford: Elsevier, 2008, pp. 97–100
- [6] W. C. Jakes, Microwave Mobile Communications, IEEE Press, 1974, p. 135
- [7] 3GPP R4-104284; Rohde & Schwarz; MIMO OTA Measurements of LTE Devices According to the Two-Channel Method; Jacksonville, http://ftp.3gpp.org/tsg_ran/WG4_Radio/, 2010-11
- [8] 3GPP R4-110646; Rohde & Schwarz; Preliminary results on LTE round robin test; Taipei, http://ftp.3gpp.org/tsg_ran/WG4_Radio/, 2011-02
- [9] 3GPP R4-111723; Rohde & Schwarz; Further results on LTE round robin devices; Shanghai, http://ftp.3gpp.org/tsg_ran/WG4_Radio/, 2011-04
- [10] 3GPP R4-112431; Rohde & Schwarz; More MIMO 3D results on LTE modems; Barcelona, http://ftp.3gpp.org/tsg_ran/WG4_Radio/, 2011-05
- [11] 3GPP R4-114052, Rohde & Schwarz; Test plan for MIMO OTA testing using two channels, Athens, http://ftp.3gpp.org/tsg_ran/WG4_Radio/, 2011-08

About Rohde & Schwarz

Rohde & Schwarz is an independent group of companies specializing in electronics. It is a leading supplier of solutions in the fields of test and measurement, broadcasting, radiomonitoring and radiolocation, as well as secure communications. Established more than 75 years ago, Rohde & Schwarz has a global presence and a dedicated service network in over 70 countries. Company headquarters are in Munich, Germany.

Environmental commitment

- Energy-efficient products
- Continuous improvement in environmental sustainability
- ISO 14001-certified environmental management system



Regional contact

Europe, Africa, Middle East

+49 89 4129 12345

customersupport@rohde-schwarz.com

North America

1-888-TEST-RSA (1-888-837-8772)

customer.support@rsa.rohde-schwarz.com

Latin America

+1-410-910-7988

customersupport.la@rohde-schwarz.com

Asia/Pacific

+65 65 13 04 88

customersupport.asia@rohde-schwarz.com

This white paper and the supplied programs may only be used subject to the conditions of use set forth in the download area of the Rohde & Schwarz website.

R&S® is a registered trademark of Rohde & Schwarz GmbH & Co. KG; Trade names are trademarks of the owners.

Rohde & Schwarz GmbH & Co. KG

Mühlhofstraße 15 | D - 81671 München

Phone + 49 89 4129 - 0 | Fax + 49 89 4129 - 13777

www.rohde-schwarz.com